C. R. Mecanique 345 (2017) 752–763

Contents lists available at ScienceDirect

Comptes Rendus Mecanique

www.sciencedirect.com

A thermo-elastoplastic model for soft rocks considering structure

Zuoyue He [a,b], Sheng Zhang [a,b,*], Jidong Teng [a,b], Yonglin Xiong [c]

[a] National Engineering Laboratory for High-Speed-Railway Construction, Central South University, China
[b] School of Civil Engineering, Central South University, Changsha 410075, China
[c] State Key Laboratory of Disaster Reduction in Civil Engineering, Tongji University, Shanghai 200092, China

ARTICLE INFO

Article history:
Received 1 April 2017
Accepted 4 July 2017
Available online 18 August 2017

Keywords:
Soft rocks
Temperature
Linear thermal expansion coefficient
Structure
Elasto-plastic

ABSTRACT

In the fields of nuclear waste geological deposit, geothermy and deep mining, the effects of temperature on the mechanical behaviors of soft rocks cannot be neglected. Experimental data in the literature also showed that the structure of soft rocks cannot be ignored. Based on the superloading yield surface and the concept of temperature-deduced equivalent stress, a thermo-elastoplastic model for soft rocks is proposed considering the structure. Compared to the superloading yield surface, only one parameter is added, i.e. the linear thermal expansion coefficient. The predicted results and the comparisons with experimental data in the literature show that the proposed model is capable of simultaneously describing heat increase and heat decrease of soft rocks. A stronger initial structure leads to a greater strength of the soft rocks. Heat increase and heat decrease can be converted between each other due to the change of the initial structure of soft rocks. Furthermore, regardless of the heat increase or heat decrease, a larger linear thermal expansion coefficient or a greater temperature always leads to a much rapider degradation of the structure. The degradation trend will be more obvious for the coupled greater values of linear thermal expansion coefficient and temperature. Lastly, compared to heat decrease, the structure will degrade more easily in the case of heat increase.

1. Introduction

In the fields of nuclear waste geological deposit, geothermy, and deep mining, the effects of temperature on the mechanical behaviors of soft rocks have attracted extensive attention [1]. The experimental data in the literature showed that these effects are complex. On the one hand, the undrained uniaxial compression tests conducted by Fujinuma et al. [2]) and Okada [3,4] showed that a temperature increase would decrease the strengths of siltstone, sandstone, and mudstone. On the other hand, the mechanical tests conducted by He [5] showed that the strengths of deep soft rocks increase with increasing temperature. Similar results were obtained by Noble [6] as well. These two different phenomena are referred to as heat decrease and heat increase by Zhang et al. [7]. Based on the subloading yield surface, Zhang et al. [7] proposed a simple thermo-elastoplastic model by introducing a concept of temperature-deduced equivalent stress. This model satisfies thermodynamic principles and can properly describe the general mechanical and thermal behavior of some typical geomaterials.

* Corresponding author at: Railway Campus of Central South University, Shaoshan South Road No. 68, Changsha, Hunan Province, 410075, China.
E-mail address: zhang-sheng@csu.edu.cn (S. Zhang).

http://dx.doi.org/10.1016/j.crme.2017.07.002
1631-0721/

However, the subloading yield surface was proposed for overconsolidated remolded soils and is not suitable for structured geomaterials [8,9].

Soft rocks are usually identified as a kind of soil with a large overconsolidated ratio [10,11]. However, soft rocks can also form structures during the sedimentation process. Xin et al. [12] found that the cementation structure of the red clay rock of Upper Pleistocene were flocculent which was then proven to be a structure through repeated shear tests. Zhang et al. [13] found that, when subjected to stress and cyclical drying/wetting, localized structural collapse of soft siltstones appeared. This type of collapse of structure would then influence the hydraulic conductivity [14]. In geologic terms, this kind of structure of soft rocks is called the random fabric structure formed in the sedimentation process, sometimes also referred to as bounding. The other kind occurs when, under the same loading, the void ratio can be maintained at a higher level than that of a non-structured soft rock because of the extra strength from the structure or bonding [15]. Through SEM and X-ray CT performed on soft carbonate rocks in Southern Italy, Ciantia et al. [16] also found that there are two distinct kinds of bonding within soft rock: temporary bonding and persistent bonding. The classification of the structure contributes to the understanding of the mechanical behavior of soft rocks. The form of the structure may be complex, so that the classification method needs to be improved in the future. To summarize, these experimental data show that the structure of soft rocks cannot be ignored and should be taken account into the mechanical model.

However, only a few models have taken the structure of soft rocks into account. Many models considering the structure are usually proposed for natural soils, but their applications to structured soft rocks are questionable [17–24]. Based on the disturbed state theory, Liu et al. [25] proposed a one-dimensional compression model for structured geomaterials, including soft rocks. This model cannot describe some complicated stress states such as triaxial compression and hollow torsional shear with drained and undrained conditions. Leroueil and Vaughan [26] investigated the effects of the structure on the strength, yield curve and compression curve of silty mudstone through drained and undrained isotropic compression tests. Based on the modified cam-clay model, several models were then proposed for structured soft rocks [27,28,15]. While these models could describe complicated stress states, the factors for the degradation of the structure were not fully analyzed.

The structure of soft rocks will be degraded by mechanical conditions during tests [29–32]. Temperature also will affect the structure of soft rocks. Wang et al. [33] found that the structure of montmorillonitic soft rocks would be nearly completely damaged at 100 °C. However, few models can describe this thermal effect on the structure of soft rocks. It is known that the concept of superloading yield surface proposed by Asaoka et al. [29] can describe structured soils properly. This concept was then adopted by Zhu et al. [15] to investigate the structure of soft rocks, which was validated using drained triaxial compression tests and triaxial creep tests. Therefore, even though this concept was initially proposed for soils, it is reasonable to adopt it in this work for the analysis of the structure effects of soft rocks. Combining the concepts of superloading yield surface and temperature-deduced equivalent stress, the effects of temperature on the degradation of the structure of soft rocks can be then analyzed.

Based on the superloading yield surface and the concept of temperature-deduced equivalent stress, a thermo-elastoplastic model considering structure for soft rocks is first proposed in this paper. Numerical simulations are then conducted to analyze the heat increase and the heat decrease of soft rocks. The proposed model is then validated by comparing the results predicted by the model with the experimental data in the literature. Finally, the effects of temperature and of the linear thermal expansion coefficient on the degradation of the structure of soft rocks are analyzed.

2. A thermo-elastoplastic model for soft rocks

When the mean stress is maintained at a constant value, the temperature increase from a reference temperature θ_0 to θ will generate a thermoelastic volumetric strain increment $\Delta\varepsilon_{\mathrm{v}}^{\mathrm{e}\theta}$. The reference temperature θ_0 is assumed to be 15 °C, representing the average global temperature. The thermoelastic volumetric strain increment is a linear function of the temperature change θ_0–θ, and can be expressed as

$$\Delta\varepsilon_{\mathrm{v}}^{\mathrm{e}\theta} = 3\alpha_{\mathrm{t}}(\theta - \theta_0) \tag{1}$$

where α_{t} is the linear thermal expansion coefficient and takes a negative value because a compressive volumetric strain is assumed as positive in geomechanics. Zhang et al. [7] suggested that the volumetric strain increment due to the temperature increment was equivalent to the volumetric strain increment caused by a certain unloading mean stress increment referred to as the equivalent stress increment

$$\begin{cases} \Delta\varepsilon_{\mathrm{v}}^{\mathrm{e}\theta} = \dfrac{\kappa}{1+e_0}\ln\dfrac{\sigma_{\mathrm{m}} + \Delta\widetilde{\sigma}_{\mathrm{m}}}{\sigma_{\mathrm{m}}} \\ \Delta\widetilde{\sigma}_{\mathrm{m}} = \sigma_{\mathrm{m}}\exp\left[\dfrac{3\alpha_{\mathrm{t}}(\theta-\theta_0)(1+e_0)}{\kappa}\right] - \sigma_{\mathrm{m}} \\ \widetilde{\sigma}_{\mathrm{m}} = \sigma_{\mathrm{m}} + \Delta\widetilde{\sigma}_{\mathrm{m}} = \sigma_{\mathrm{m}}\exp\left[\dfrac{3\alpha_{\mathrm{t}}(\theta-\theta_0)(1+e_0)}{\kappa}\right] \end{cases} \tag{2}$$

where σ_{m} is mean stress, i.e. $\sigma_{\mathrm{m}} = p = \sigma_{ii}/3$, $\Delta\widetilde{\sigma}_{\mathrm{m}}$ is the equivalent stress increment, $\widetilde{\sigma}_{\mathrm{m}}$ is the equivalent stress, κ is the swelling index and e_0 is the void ratio in the reference state when the reference stress is assumed to be a standard

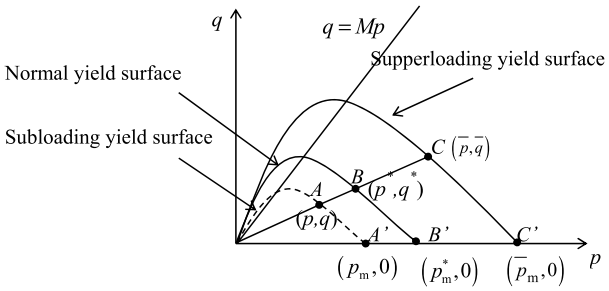

Fig. 1. Stress states and yield surfaces of soils.

atmospheric pressure, i.e. 98 kPa. Therefore, considering the temperature effect, the reference states in this paper include both the temperature state and the stress state.

The superloading surface, which is similar in shape to the original Cam–clay yield surface, is located above the Cam–clay yield surface and the size ratio between two yield surfaces gives the degree of the structure of soil skeleton, as shown in Fig. 1. According to Asaoka et al. [29], the superloading concept is given by

$$\begin{cases} f_{\mathrm{s}} = \ln\dfrac{p}{p_{\mathrm{m}}} + \dfrac{1}{M}\dfrac{q}{p} = 0 \\ f = \ln\dfrac{p^*}{p^*_{\mathrm{m}}} + \dfrac{1}{M}\dfrac{q^*}{p^*} = 0 \\ f_{\mathrm{u}} = \ln\dfrac{\overline{p}}{\overline{p}_{\mathrm{m}}} + \dfrac{1}{M}\dfrac{\overline{q}}{\overline{p}} = 0 \end{cases} \tag{3}$$

where f_{s}, f and f_{u} are subloading yield surface, normal yield surface and superloading yield surface, respectively. p and q are the mean stress and deviator stress, respectively. M is the ratio of shearing stress at critical state. $R = p_{\mathrm{m}}/\overline{p}_{\mathrm{m}} = p/\overline{p} = q/\overline{q} = 1/\mathrm{OCR}$ is the state variable for the overconsolidated ratio and $R^* = p^*_{\mathrm{m}}/\overline{p}_{\mathrm{m}} = p^*/\overline{p} = q^*/\overline{q}$ is the state variable for the soil structure. An increase in the state variable R^* represents a weakening of the soil structure, and $R^* = 1.0$ represents no structure, i.e. the soil is remolded soil. $\varepsilon^{\mathrm{p}}_{\mathrm{v}} = C_{\mathrm{p}} \ln(p^*_{\mathrm{m}}/p^*_0)$ is the isotropic compression plastic strain of normal consolidated geomaterials. C_{p} is equal to $(\lambda-\kappa)/(1+e_0)$. p^*_0 is the reference stress state. $p_{\mathrm{m}} = p\exp(q/M/p)$, $p^*_{\mathrm{m}} = p^*_0\exp(\varepsilon^{\mathrm{p}}_{\mathrm{v}}/C_{\mathrm{p}})$ and $\overline{p}_{\mathrm{m}} = p^*_{\mathrm{m}}/R^*$ are the values of the crossing points of the p axis with the subloading yield surface, the normal yield surface and the superloading yield surface, respectively. (p,q), (p^*,q^*) and $(\overline{p},\overline{q})$ are the present stress state, normal consolidation stress state and structure stress state, respectively. The subloading yield surface is also geometrically similar to the normal yield surface and passes through the present stress state and changes with the stress, which means all of the present stresses located at the surface [8]. Therefore, it is not needed to determine whether the stress state reaches the yield surface by using this concept to deduce the loading criterion.

It is assumed that the structured soil consolidation lines (SCL) are geometrically similar. The void ratio moves upward with increasing temperature, implying that the soil volume or void ratio increases, as shown in Fig. 2. In plane $\theta_0 = \theta$, the following equations can be obtained

$$\begin{cases} \widetilde{p}^*_0 = p_0\exp\left[\dfrac{3\alpha_{\mathrm{t}}(\theta-\theta_0)(1+e_0)}{\kappa}\right] = p^*_0 \\ \widetilde{p}^*_{\mathrm{m}} = p^*_{\mathrm{m}}\exp\left[\dfrac{3\alpha_{\mathrm{t}}(\theta-\theta_0)(1+e_0)}{\kappa}\right] = p^*_{\mathrm{m}} \\ \widetilde{\overline{p}}_{\mathrm{m}} = \overline{p}_{\mathrm{m}}\exp\left[\dfrac{3\alpha_{\mathrm{t}}(\theta-\theta_0)(1+e_0)}{\kappa}\right] = \overline{p}_{\mathrm{m}} \\ \widetilde{p}_{\mathrm{m}} = p_{\mathrm{m}}\exp\left[\dfrac{3\alpha_{\mathrm{t}}(\theta-\theta_0)(1+e_0)}{\kappa}\right] = p_{\mathrm{m}} \end{cases} \tag{4}$$

The symbol $\sim$ represents the effect of temperature. The equivalent stress $\widetilde{p}_{\mathrm{m},i}$ $(i=0,1,2)$ corresponds to the subloading yield surface and $\theta_0 < \theta_1 < \theta_2$, $\widetilde{p}_{\mathrm{m},0} < \widetilde{p}_{\mathrm{m},1} < \widetilde{p}_{\mathrm{m},2}$. $\widetilde{\overline{p}}_{\mathrm{m},i}$ $(i=0,1,2)$ corresponds to the superloading yield surface and $\theta_0 < \theta_1 < \theta_2$, $\widetilde{\overline{p}}_{\mathrm{m},0} < \widetilde{\overline{p}}_{\mathrm{m},1} < \widetilde{\overline{p}}_{\mathrm{m},2}$. To simplify the expression, the equations are merged to give:

$$\begin{aligned} &\widetilde{p}_{\mathrm{m},i} = p_{\mathrm{m}}(\theta_i) \\ &\widetilde{\overline{p}}_{\mathrm{m},i} = \overline{p}_{\mathrm{m}}(\theta_i) \end{aligned} \quad (i = 0, 1, 2\ldots) \tag{5}$$

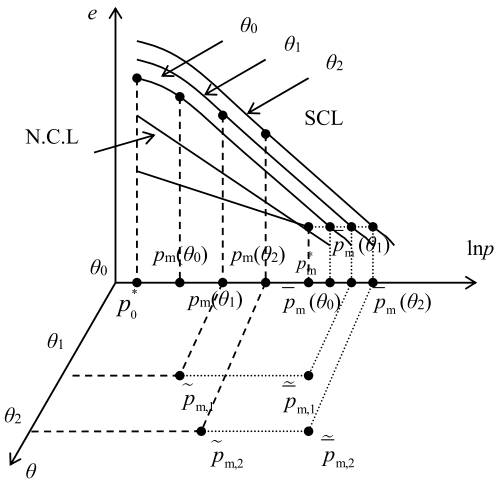

Fig. 2. Effects of temperature change on SCL.

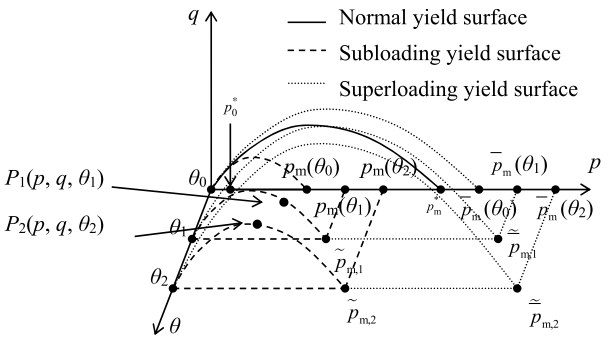

Fig. 3. Effects of temperature change on subloading and superloading surfaces.

Similar to the treatment for superloading yield surface without considering the temperature, it is assumed that subloading yield surfaces, normal yield surfaces, and superloading yield surfaces are also geometrically similar. The three kinds of yield surface changes with temperature in the p–q–θ plane are shown in Fig. 3. It can be observed that both the subloading yield surface and the superloading yield surface expand outward with increasing temperature. The superloading yield surface is proposed for overconsolidated natural soils, implying that under the present stress state, a kind of soil is in the overconsolidated state. However, the normal yield surface is proposed for the normal consolidated remolded soils and can be obtained by the triaxial test at room temperature. The normal yield surface is the reference surface in this paper and does not change with temperature [7].

It is assumed that the definitions of the overconsolidated state variable and the structure state variable remain unchanged when the temperature is considered. The stress is replaced by the equivalent stress and then the following equations can be obtained

$$\begin{aligned}\widetilde{R} &= \widetilde{p}_{\mathrm{m}}/\widetilde{\overline{p}}_{\mathrm{m}} \\ \widetilde{R}^{*} &= \widetilde{p}^{*}_{\mathrm{m}}/\widetilde{\overline{p}}_{\mathrm{m}}\end{aligned} \tag{6}$$

when $\theta=\theta_0$, $\widetilde{R}=\widetilde{p}_{\mathrm{m},0}/\widetilde{\overline{p}}_{\mathrm{m},0}$ and $\widetilde{R}^{*}=\widetilde{p}^{*}_{\mathrm{m},0}/\widetilde{\overline{p}}_{\mathrm{m},0}$; when $\theta=\theta_1$, $\widetilde{R}=\widetilde{p}_{\mathrm{m},1}/\widetilde{\overline{p}}_{\mathrm{m},1}$ and $\widetilde{R}^{*}=\widetilde{p}^{*}_{\mathrm{m},1}/\widetilde{\overline{p}}_{\mathrm{m},1}$; when $\theta=\theta_2$, $\widetilde{R}=\widetilde{p}_{\mathrm{m},2}/\widetilde{\overline{p}}_{\mathrm{m},2}$ and $\widetilde{R}^{*}=\widetilde{p}^{*}_{\mathrm{m},2}/\widetilde{\overline{p}}_{\mathrm{m},2}$. At the present stress state, the subloading yield surface of the superloading concept considering the temperature can then be expressed as [7]

$$f_{\mathrm{s}}=\ln\frac{p}{\widetilde{p}_{\mathrm{m}}}+\frac{1}{M}\frac{q}{p}=0 \tag{7}$$

Substituting Eq. (6) into Eq. (7), it can then be rewritten as

$$f_{\mathrm{s}}=\ln\frac{p}{\widetilde{p}^{*}_{\mathrm{m}}}+\frac{1}{M}\frac{q}{p}+\ln\widetilde{R}^{*}-\ln\widetilde{R}=0 \tag{8}$$

Substituting Eq. (4) into Eq. (8), it can then be rewritten as

$$\begin{aligned}f_{\mathrm{s}}&=\ln\frac{p}{\widetilde{p}^{*}_{\mathrm{m}}}+\frac{1}{M}\frac{q}{p}+\ln\widetilde{R}^{*}-\ln\widetilde{R}=\ln\frac{p}{p^{*}_{0}}+\frac{1}{M}\frac{q}{p}+\ln\widetilde{R}^{*}-\ln\widetilde{R}-\ln\frac{p^{*}_{\mathrm{m}}}{p^{*}_{0}} \\ &=\ln\frac{p}{p^{*}_{0}}+\frac{1}{M}\frac{q}{p}+\ln\widetilde{R}^{*}-\ln\widetilde{R}-\frac{\varepsilon^{\mathrm{p}}_{\mathrm{v}}}{C_{\mathrm{p}}}=0\end{aligned} \tag{9}$$

Therefore, in the general stress space at the present stress state, Eq. (9) can be rewritten as

$$f=f_{\mathrm{s}}=\ln\frac{\sigma_{\mathrm{m}}}{\sigma^{*}_{\mathrm{m0}}}+\frac{\sqrt{3}}{M}\frac{\sqrt{J_2}}{\sigma_{\mathrm{m}}}+\ln\widetilde{R}^{*}-\ln\widetilde{R}-\frac{1}{C_{\mathrm{p}}}\varepsilon^{\mathrm{p}}_{\mathrm{v}}=0 \tag{10}$$

where J_2 is the second invariant of the deviatoric stress tensor. σ^{*}_{m0} is the reference stress state and is the same as p^{*}_{0}.

The consistency equation is given by

$$\mathrm{d}f=0 \quad\Rightarrow\quad \frac{\partial f}{\partial\sigma_{ij}}\mathrm{d}\sigma_{ij}+\frac{\partial f}{\partial\widetilde{R}^{*}}\mathrm{d}\widetilde{R}^{*}-\frac{\partial f}{\partial\widetilde{R}}\mathrm{d}\widetilde{R}-\frac{1}{C_{\mathrm{p}}}\mathrm{d}\varepsilon^{\mathrm{p}}_{\mathrm{v}}=0 \tag{11}$$

The associated flow rule is adopted in this paper, which means that the proposed yield function is the same as the thermoplastic potential. Therefore, the plastic strain increment can be calculated as

$$\mathrm{d}\varepsilon_{ij}^{\mathrm{p}} = \Lambda \frac{\partial f}{\partial \sigma_{ij}}, \qquad \mathrm{d}\varepsilon_{\mathrm{v}}^{\mathrm{p}} = \Lambda \frac{\partial f}{\partial \sigma_{ii}} \tag{12}$$

where Λ is a non-negative parameter. The first-order partial derivatives of the structure state variable and the overconsolidated state variable can then be obtained as

$$\frac{\partial f}{\partial \widetilde{R}^*} = \frac{1}{\widetilde{R}^*}, \qquad \frac{\partial f}{\partial \widetilde{R}} = \frac{1}{\widetilde{R}} \tag{13}$$

The structure state variable and the overconsolidated state variable are closely related to the plastic strain and can be written as [34,29–31]

$$\begin{cases} \mathrm{d}\widetilde{R} = U_e \mathrm{d}\varepsilon_{\mathrm{d}}^{\mathrm{p}} \\ \mathrm{d}\widetilde{R}^* = U_{\mathrm{e}}^* \mathrm{d}\varepsilon_{\mathrm{d}}^{\mathrm{p}} \\ U_{\mathrm{e}} = -m_{\widetilde{R}} \ln \widetilde{R} \dfrac{M}{C_{\mathrm{p}}} \\ U_{\mathrm{e}}^* = \widetilde{R}^* \left[1 - \left(\widetilde{R}^*\right)^{m_{\widetilde{R}^*}}\right] \dfrac{M}{C_{\mathrm{p}}} \end{cases} \tag{14}$$

where $m_{\widetilde{R}^*}$ and $m_{\widetilde{R}}$ are material parameters and control the degradations of the structure state variable and the overconsolidated state variable, respectively. The two material parameters are intrinsic characteristics of structure geomaterials, which means that the two material parameters do not change with temperature. $\widetilde{R}$ and $\widetilde{R}^*$ are obviously related to temperature, as seen in Eq. (6), so $\mathrm{d}\widetilde{R}$ and $\mathrm{d}\widetilde{R}^*$ are also influenced by temperature.

The plastic shear strain increment $\mathrm{d}\varepsilon_{\mathrm{d}}^{\mathrm{p}}$ is given by

$$\mathrm{d}\varepsilon_{\mathrm{d}}^{\mathrm{p}} = \sqrt{\frac{2}{3}} \sqrt{\mathrm{d}e_{ij}^{\mathrm{p}} \mathrm{d}e_{ij}^{\mathrm{p}}} = \Lambda \sqrt{\frac{2}{3}} \left| \frac{\partial f}{\partial s_{ij}} \right| \tag{15}$$

s_{ij} is the deviatoric stress tensor. Additional equations for solving the proposed model are written as

$$\begin{cases} \dfrac{\partial f}{\partial \sigma_{\mathrm{mm}}} = \dfrac{1}{\sigma_{\mathrm{m}}} - \dfrac{\sqrt{3}}{M} \dfrac{\sqrt{J_2}}{\sigma_{\mathrm{m}}^2} \\ \dfrac{\partial f}{\partial s_{ij}} = \dfrac{\sqrt{3}}{2M\sigma_{\mathrm{m}}} \dfrac{s_{ij}}{\sqrt{J_2}} \\ \dfrac{\partial f}{\partial \sigma_{ij}} = \dfrac{\partial f}{\partial s_{ij}} + \dfrac{\partial f}{\partial \sigma_{\mathrm{mm}}} \dfrac{\delta_{ij}}{3} \end{cases} \tag{16}$$

Considering the temperature factor, the first expression of Eq. (16) can be rewritten as

$$\left| \frac{\partial f}{\partial s_{ij}} \right| = \frac{1}{M} \frac{1}{\widetilde{\sigma}_{\mathrm{m}}} \sqrt{\frac{3}{2}} = \frac{1}{M} \frac{1}{\sigma_{\mathrm{m}} \exp\left[\frac{3\alpha_{\mathrm{t}}(\theta-\theta_0)(1+e_0)}{\kappa}\right]} \sqrt{\frac{3}{2}} \tag{17}$$

Substituting Eqs. (12), (13), (14), (15), (16) and (17) into Eq. (9), the consistency equation can then be rewritten as

$$\frac{\partial f}{\partial \sigma_{ij}} \mathrm{d}\sigma_{ij} + \left\{ \left[1 - \left(\widetilde{R}^*\right)^{m_{\widetilde{R}^*}}\right] + \frac{m_{\widetilde{R}} \ln \widetilde{R}}{\widetilde{R}} \right\} \frac{1}{C_{\mathrm{p}} \sigma_{\mathrm{m}} \exp\left[\frac{3\alpha_{\mathrm{t}}(\theta-\theta_0)(1+e_0)}{\kappa}\right]} \Lambda - \frac{1}{C_{\mathrm{p}}} \Lambda \frac{\partial f}{\partial \sigma_{\mathrm{mm}}} = 0 \tag{18}$$

Based on the Hooke's law, the incremental stress tensor can be obtained as

$$\mathrm{d}\sigma_{ij} = E_{ijkl} \mathrm{d}\varepsilon_{\mathrm{kl}}^{\mathrm{e}\sigma} = E_{ijkl} \left(\mathrm{d}\varepsilon_{kl} - \mathrm{d}\varepsilon_{kl}^{\mathrm{p}} - \mathrm{d}\varepsilon_{kl}^{\mathrm{e}\theta}\right) = E_{ijkl} \mathrm{d}\varepsilon_{kl} - E_{ijkl} \frac{\partial f}{\partial \sigma_{kl}} \Lambda - E_{ijkl} \cdot 3\alpha_{\mathrm{t}} \delta_{kl} \mathrm{d}\theta \tag{19}$$

where E_{ijkl} is a fourth-order stiffness tensor. By substituting Eq. (17) into Eq. (16), the non-negative parameter Λ can be obtained

$$\Lambda = \frac{\frac{\partial f}{\partial \sigma_{ij}} E_{ijkl} \mathrm{d}\varepsilon_{kl} - \frac{\partial f}{\partial \sigma_{ij}} E_{ijkl} 3\alpha_{\mathrm{t}} \delta_{kl} \mathrm{d}\theta}{h^{\theta} + \frac{\partial f}{\partial \sigma_{ij}} E_{ijkl} \frac{\partial f}{\partial \sigma_{kl}}} \tag{20}$$

where

Table 1
Mechanical properties and material parameters.

Number	α_t (1/°C)	ν	M	λ	κ	OCR	p_i (MPa)	$m_{\widetilde{R}}$	$m_{\widetilde{R}^*}$	$\widetilde{R}^*$
1	−3.0e−6	0.110	1.876	0.0115	0.0015	110.0	0.5	0.15	0.01	0.01
2	−2.0e−5	0.200	1.269	0.0225	0.0100	160.0	1.0	0.01	1	0.35
3	−2.0e−5	0.200	1.269	0.0225	0.0100	10.0	1.5	0.1	1	0.25 0.65
4	−3.0e−6	0.110	1.876	0.0115	0.0015	110.0	0.5	0.38	0.23	0.25
5	−2.0e−5	0.150	1.269	0.23	0.189	1	0.05	2.5	0.31	1

$$\begin{cases} h^{\theta} = \dfrac{1}{C_p M \sigma_m}(M_s - \eta), \qquad \eta = \dfrac{\sqrt{3}\sqrt{J_2}}{\sigma_m} \\ M_s = \left\{1 - \dfrac{[1-(\widetilde{R}^*)^{m_{\widetilde{R}^*}}] + \frac{m_{\widetilde{R}} \ln \widetilde{R}}{\widetilde{R}}}{\exp[\frac{3\alpha_t(\theta-\theta_0)(1+e_0)}{\kappa}]}\right\} M \end{cases} \tag{21}$$

The loading criteria are given in the same way as in the previous work by Zhang et al. [10] as

$$\begin{aligned} &\left\| \mathrm{d}\varepsilon_{ij}^{p\sigma} \right\| > 0 \quad \text{if } \Lambda > 0 \quad \text{and} \quad \begin{cases} \frac{\partial f}{\partial \sigma_{ij}} \mathrm{d}\sigma_{ij} > 0 \text{ hardening.} \\ \frac{\partial f}{\partial \sigma_{ij}} \mathrm{d}\sigma_{ij} < 0 \text{ softening} \end{cases} \\ &\left\| \mathrm{d}\varepsilon_{ij}^{p\sigma} \right\| = 0 \quad \text{if } \Lambda \le 0 \quad \text{elastic} \end{aligned} \tag{22}$$

3. Heat increase and heat decrease

As we can know from the previous sections, soft rocks show two different mechanics due to temperature, the so-called heat increase and heat decrease. For demonstrating that the proposed model in this paper can describe the two different mechanics, an analysis example for drainage triaxial compression test is performed. All mechanical parameters and material parameters of soft rocks are shown in Table 1. ν is the Poisson ratio, M is the ratio of the shearing stress at the critical state, λ is the compression index, κ is the swelling index, p_i is the initial stress, and e_0 is the void ratio in the reference state and takes a value of 0.72. 20 °C and 90 °C are adopted in this paper, representing room temperature and high temperature, respectively. The simulated results are shown in Fig. 4(a) and (b) and the parameters correspond to the first and the second entries in Table 1, respectively. With increasing temperature, it can be observed that the strength decreases shown in Fig. 4(a) and then increases shown in Fig. 4(b), which present the heat decrease and heat increase, respectively. It is notable that the material properties in the two cases are different, which means that there are two different kinds of soft rocks. For the same soft rock, the dual effect of temperature can also occur as shown in Fig. 4(b). The parameters are all the same. When temperature increases from 90 °C to 95 °C, the strength decreases slightly. This implies that there might be an optimum temperature for soft rocks at which the strength will reach the maximum value. However, it should be noted that this optimum temperature is just a theoretical prediction that has to be validated with sufficient tests. In a word, the results demonstrate that the model proposed in this paper can simultaneously describe the two different mechanics of soft rocks subjected to temperature.

The experimental data in the literature are also used to validate the proposed model. Zhang et al. [7] performed thermal triaxial compression tests for Ohya stone using a novel temperature-controlled triaxial compression test device. For safety, the highest temperature within the chamber was set at 90 °C during the test. The height and diameter of the cylindrical test specimen are 100 mm and 50 mm, respectively. Isotropic consolidation was conducted for 24 h under the prescribed confining pressure and temperature. The rate of temperature increase was set at 0.5 °C/min under drained conditions, and then the target temperature was kept constant for 1 h. The shearing rate was set at 0.001%/min under drained conditions and at the target temperature. The mechanical parameters and material parameters of Ohya stone are listed in entry 4 in Table 1. The initial structure state variable of Ohya stone takes a value of 0.25, corresponding to a strong structure. Comparisons between the predicted and experimental results are shown in Fig. 5. It can be seen that the model predictions are in good agreement with the experimental results. The peak of axial stress at 80 °C is less than that at 20 °C, corresponding to a heat decrease.

Unfortunately, there are not enough experimental results and predicted results on the heat increase of soft rocks in the literature. Although the test conducted by He [5] showed that a heat increase appeared, only one graph was given to depict the stress–strain relationship without describing the test process. The mechanical and material parameters such as the Poisson ratio, the ratio of shearing stress at critical state, the compression index, the swelling index, the overconsolidated ratio, and the initial stress were not specified. These parameters are necessary inputs for the prediction by the proposed model. Similarly, Noble [6] simply theoretically analyzed the soft rocks' heat increase. The thermal-elastoplastic model proposed by Zhang et al. [7] is capable of uniformly describing heat increase and heat decrease of geomaterials, including soft rocks. The effects of mechanical parameters and material parameters on these two different types of thermodynamics were also

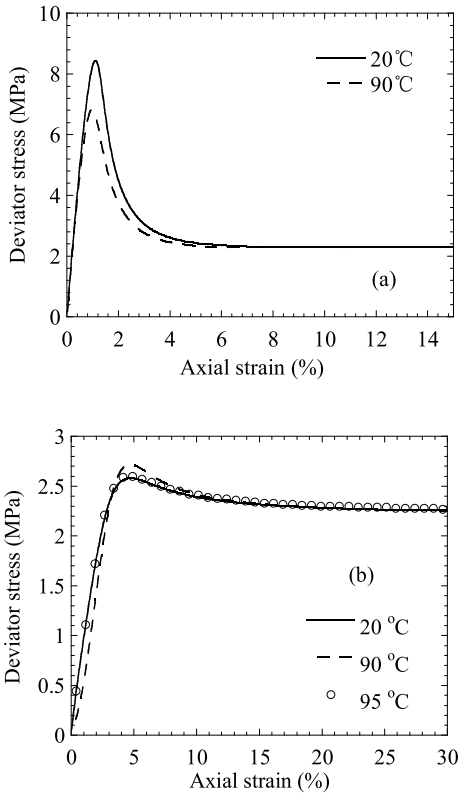

Fig. 4. Soft rocks: (a) heat decrease and (b) heat increase.

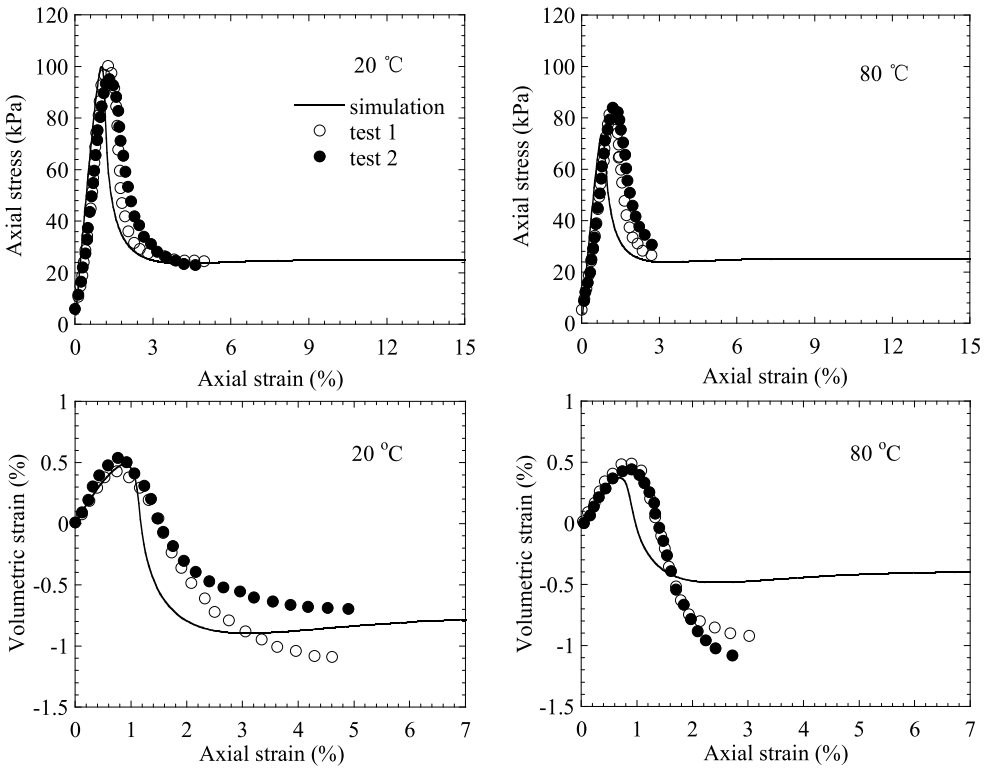

Fig. 5. Comparisons between theoretical and experimental results.

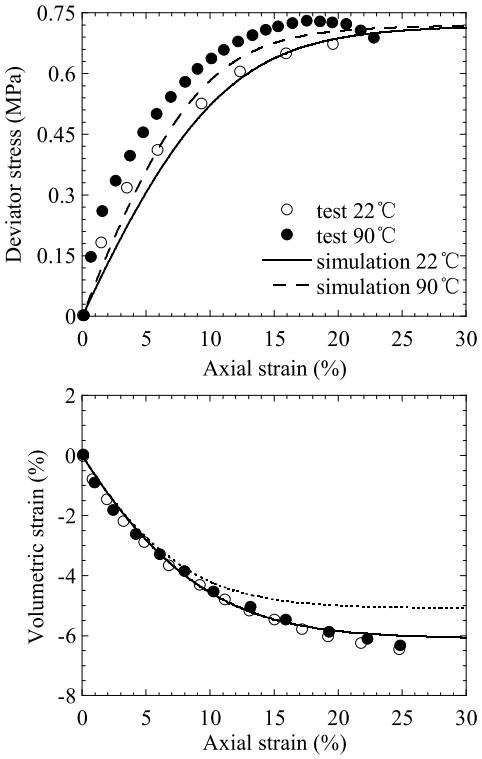

Fig. 6. Comparisons between theoretical and experimental results.

analyzed in detail. However, only the heat decrease of soft rocks was validated by the thermal triaxial compression tests for Ohya stone.

The work by Cekerevac and Laloui [35] was employed to validate the heat increase predicted by the model proposed in this paper. Samples of CM clay were prepared by mixing de-aired distilled water with clay powder in the presence of a water content that was two times higher than the liquid limit. Isotropic consolidation of the slurry was then carried out under a confining pressure of 100 kPa. These samples were 110 mm in height and 55 mm in diameter. The drained triaxial compression tests were performed at two different temperatures (22 °C and 90 °C) using a new temperature-controlled triaxial device. The initial confining pressure was set at 600 kPa to quantify the effect of the temperature on the shear strength of the CM clay. The initial overconsolidated ratio and the initial structure were both 1, because these samples were prepared by normal consolidated remolded CM clay. The mechanical and material parameters of the CM clay are listed in entry 5 in Table 1. The comparison between the predicted and experimental results is shown in Fig. 6. It can be observed that the predictions are in good agreement with the experimental results. The results also indicate that the samples tested at high temperature show higher strength, corresponding to the heat increase. However, due to the lack of sufficient tests results in the literature, the predicted results for the CM clay do not demonstrate that the model proposed in this paper can also predict the heat increase of soft rocks well. Future experimental studies of soft rocks still need to pay much more attention to heat increase.

4. Effects of linear thermal expansion coefficient and temperature on soft rocks' structure

The linear thermal expansion coefficient and target temperature are two important temperature factors for the thermodynamics of soft rocks. The effects of these two parameters on the evolution of the structure state variable are shown in Figs. 7 and 8, corresponding to Figs. 4(a) and 4(b), respectively. It can be seen that regardless of the heat increase or heat decrease, in the case of a lower temperature, the structure state variable degrades more quickly with the linear thermal expansion coefficient increasing. A temperature increase can aggravate this trend, meaning that the structure state variable will degrade remarkably with increasing linear thermal expansion coefficient. For example, the structure state variable has already degraded completely at 90 °C and −2.0e–6 1/°C before the axial strain reaches 5%, which is much lower than that in other cases. When the linear thermal expansion coefficient is lower, the structure state variable also degrades more quickly with increasing temperature. The linear thermal expansion coefficient increase can also aggravate this trend, implying that the structure state variable will degrade remarkably with increasing temperature. To summarize, Figs. 7 and 8 show that the increase in either the linear thermal expansion coefficient or temperature can both lead to a quicker degradation, with this trend becoming more obvious when both parameters are larger.

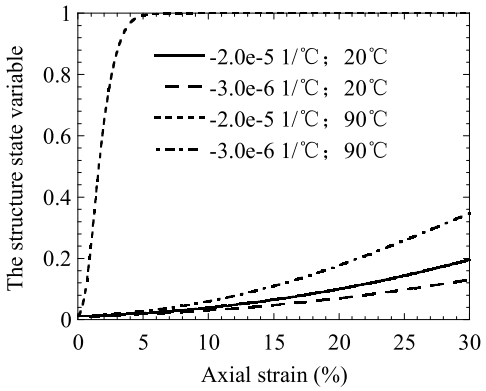

Fig. 7. Degradation of the state variable $\widetilde{R}^*$ of structure (heat decrease).

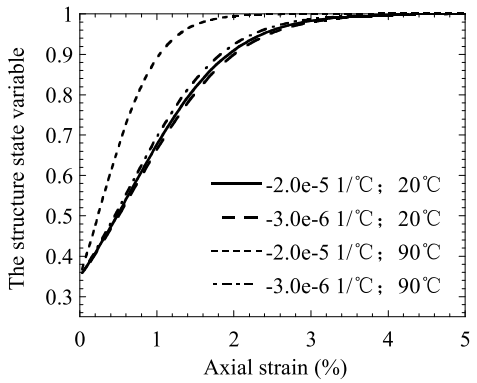

Fig. 8. Degradation of the state variable $\widetilde{R}^*$ of structure (heat increase).

Figs. 7 and 8 also show that compared to heat decrease, the slope of the structure state variable curve is much larger, despite the changes in the linear thermal expansion coefficient and temperature. Therefore, the structure state variable in the case of a heat increase degrades more quickly than that in the case of a heat decrease. For example, the structure state variable degrades completely before the axial strain reaches 5% in the case of the heat increase. However, in the case of the heat decrease, the structure state variable is still relatively strong, even though the axial strain reaches 30%. Even if the linear thermal expansion coefficient and the temperature are both larger, the axial strain is still slightly greater than 5% when the structure state variable degrades completely. It can be concluded that for soft rocks, the degradation rates of the structure state variable are completely different in the cases of heat increase and heat decrease.

Based on the results of this work, the structure of soft rocks is represented by the structure state variable in the super-loading yield surface. It is necessary to study both the effect of the initial structure state variable on the thermodynamics of soft rocks and the effect of the temperature on the evolution of the structure state variable. A calculation example is then examined by the proposed model to analyze these effects. The initial structure state variable takes values of 0.25 and 0.65, representing a strong and a weak structure, respectively. The mechanical and material parameters of soft rocks are listed in entry 3 in Table 1. The predicted results are shown in Fig. 9(a). It can be observed that a heat increase appears with a strong structure, while a heat decrease appears with a weak structure. The heat increase can switch to a heat decrease when the initial structure state variable varies from a small value to a large one. From the results presented in the previous sections, we can know that heat increase and heat decrease are the multiple working results of the initial overconsolidated state variable, the initial structure state variable and temperature. This calculation example demonstrates this multiple effect from the standpoint of the initial structure state variable.

Generally speaking, the strength of soft rocks increases with the increasing initial structure state variable. However, Fig. 9(a) shows that when the initial structure state variable takes a value of 0.25, the strength is slightly smaller than that when the initial structure state variable is 0.65. This seems contradictory and puzzling. It is notable that, even though the other parameters are same, the values of the initial structure state variable are different in this calculation example, implying that the initial physical states are also different. The two values of the initial structure state variable essentially represent two different kinds of soft rocks. Therefore, for different kinds of soft rocks, the conclusions obtained based on Fig. 9(a) cannot represent those for the same kind of soft rocks. The other calculation example is then conducted using the model proposed in this paper to analyze the same kinds of soft rocks. The initial overconsolidated ratios are 4 and 1.54, corresponding to the values of the initial structure state variable. Therefore, the two cases in this new calculation example have the same $\widetilde{p}_{\mathrm{m}}$, which means that the soft rocks in these two cases are just two different initial states of one kind of soft rock. The other mechanical and material parameters are all the same as those in Fig. 9(a). The predicted results are shown in Fig. 9(b). It can be observed that when the initial structure state variable takes a value of 0.25, the strength is larger than that when the initial structure state variable is 0.65. Heat increase and heat decrease can also switch to each other with the changes of the structure state variable.

The degradation curves of the two different kinds of soft rocks and the same kind of soft rock are shown in Figs. 10 and 11, corresponding to Figs. 9(a) and 9(b), respectively. It can be seen that increasing temperature can lead to a more rapid degradation of the structure state variable in all cases, even though this kind of accelerating effect is not relatively obvious. The degradation curves of the two different kinds of soft rocks are nearly the same as that of the same kind of soft rock. Therefore, the degradation of the structure state variable appears to have no direct relationship with the initial overconsolidated ratio. Furthermore, the slope in the case of a strong initial structure (heat increase) is greater than that for a weak initial structure (heat decrease). This means that compared to heat decrease, the structure state variable degrades more rapidly in the case of a heat increase, in agreement with the previous analysis. It is also notable that the structure state variable degrades completely when the initial structure is weak, prior to that in the case of a strong initial structure (heat increase). This appears to differ from the previous analysis. A reasonable origin for this is that the initial structure is so weak that the structure will degrade completely within a short time, even though the degradation rate is low. The conclusion that

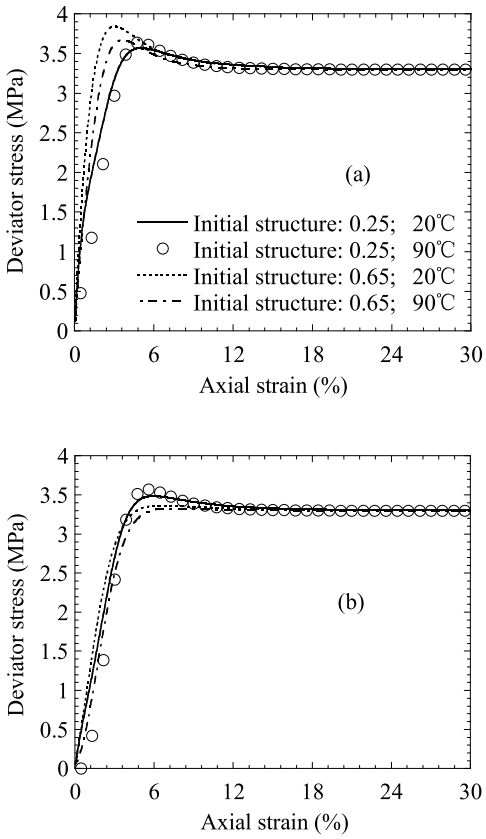

Fig. 9. Effects of the initial structure on the strength of soft rocks.

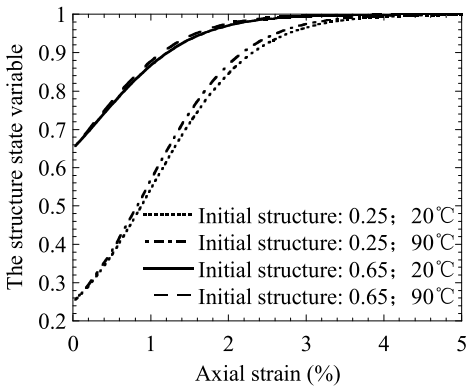

Fig. 10. Degradation of state variable $\widetilde{R}^*$ of structure: different kinds of soft rock.

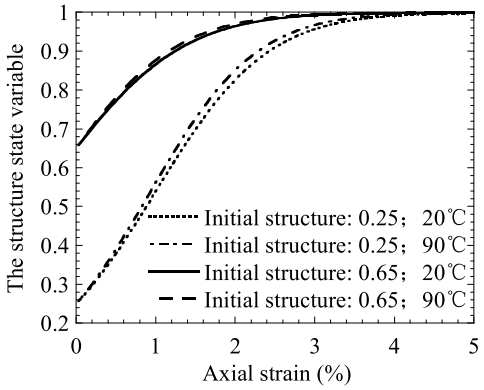

Fig. 11. Degradation of the state variable $\widetilde{R}^*$ of structure: the same kind of soft rock.

the structure degrades more rapidly in the case of the heat increase still holds. Based on the two calculation examples, it can also be concluded that the degradation of the structure state variable is related to both the initial mechanical conditions and the initial physical and mechanical properties, corresponding to Eq. (14).

Heat increase and heat decrease of soft rocks are the result of the coupled effects of overconsolidated ratio, structure, and temperature. On the one hand, generally speaking, a temperature increase can generate a larger overconsolidated ratio [7]. A larger initial overconsolidated ratio or a stronger initial structure can lead to a greater strength. On the other hand, from the previous sections, it can be known that the initial structure degrades more quickly with the increase of temperature in this case and then reduces the strength of soft rocks. A temperature increase can also decrease the overconsolidated ratio [7]. Soft rocks exhibit a heat increase when the first case dominates, while a heat decrease appears when the second case dominates. For example, in the case of a weak initial structure, the strength of soft rocks decreases with increasing

temperature (Fig. 9). However, in the case of a strong initial structure, the strength of soft rocks increases with increasing temperature (Fig. 9).

The overconsolidated ratio and material parameters controlling the degradations of the structure state variable and the overconsolidated state variable and other parameters can also influence the stress/strain relationship of certainly, which has been analyzed by Zhang et al. [7]. However, the main research of this paper focuses on temperature effects and structure of soft rocks. Therefore, these parameters are not analyzed in this paper.

5. Conclusions

Based on the superloading yield surface and the concept of temperature-deduced equivalent stress, a thermo-elastoplastic model considering the structure of soft rocks is proposed in this paper. Only one new parameter, namely, the linear thermal expansion coefficient, is added in the proposed model. Based on the model predictions and the comparisons with experimental data in the literature, we present some concluding remarks as follows.

(1) Heat increase and heat decrease are the coupled effects of the initial overconsolidated state variable, the initial structure state variable, and temperature. A larger initial overconsolidated ratio or a stronger initial structure can lead to a greater strength. A temperature increase can accelerate the degradation rates of both the initial overconsolidated ratio and the initial structure, reducing the strength of soft rocks. Soft rocks undergo heat decrease when the first case dominates, while a heat increase appears when the second case dominates.

(2) The model proposed in this paper is capable of uniformly describing both heat increase and heat decrease. Comparisons to experimental data in the literature also validate the proposed model. For the same kind of soft rock, the strength increases with the increase of the initial structure. Heat increase and heat decrease behaviors can switch to each other based on the changes in the initial structure state variable.

(3) Regardless of heat increase or heat decrease, the structure state variable always degrades more rapidly with increasing linear thermal expansion coefficient and temperature. This trend will be more obvious when both the linear thermal expansion coefficient and temperature are larger.

(4) Compared to the heat decrease, the slope of the structure state variable is sharper, which means that the structure tends to degrade more rapidly in the case of the heat increase.

Acknowledgements

This research was supported by the National Basic Research Program of China (No. 2014CB047001) and the National Natural Science Foundation of China (No. 51508578).

References

[1] S. Zhang, F. Zhang, A thermo-elasto-viscoplastic model for soft sedimentary rock, Soil Found. 49 (4) (2009) 583–595.
[2] S. Fujinuma, T. Okada, S. Hibino, et al., Consolidated undrained triaxial compression test of sedimentary soft rock at a high temperature, in: Proceedings of the 32nd Symposium on Rock Mechanics, Japan, 2003, pp. 125–130 (in Japanese).
[3] T. Okada, Mechanical properties of sedimentary soft rock at high temperatures (part 1), in: Evaluation of Temperature Dependency Based on Triaxial Compression Test, Denryoku Chuo Kenkyusho Hokoku, 2005, pp. 1–4.
[4] T. Okada, Mechanical properties of sedimentary soft rock at high temperatures (part 2), in: Evaluation of Temperature Dependency of Creep Behavior Based on Unconfined Compression Test, Denryoku Chuo Kenkyusho Hokoku, 2006, pp. 1–4.
[5] M.C. He, Progress and challenges of soft rock engineering in depth, J. China Coal Soc. 39 (8) (2014) 1409–1417 (in Chinese).
[6] C.A. Noble, Effect of Temperature on Strength of Soils, Iowa State University, Iowa, USA, 1968.
[7] S. Zhang, W.M. Leng, F. Zhang, et al., A simple thermo-elastoplastic model for geomaterials, Int. J. Plast. 34 (2012) 93–113.
[8] K. Hashiguchi, M. Ueno, Elasto-plastic constitutive laws of granular materials, constitutive equations of soils, in: Proc. Spec. Session 9 of 9th Int. ICSMFE, 1977, pp. 73–82.
[9] T. Nakai, M. Hinokio, A simple elastoplastic model for normally and over consolidated soils with unified material parameters, Soil Found. 44 (2) (2004) 53–70.
[10] F. Zhang, A. Yashima, T. Nakai, et al., An elasto-viscoplastic model for soft sedimentary rock based on t_{ij} concept and subloading yield surface, Soil Found. 45 (2005) 65–73.
[11] S. Zhang, S. Xu, J. Teng, et al., Effect of temperature on the time-dependent behavior of geomaterials, C. R. Mecanique 344 (8) (2016) 603–611.
[12] P. Xin, S.R. Wu, S.J. Shi, et al., Structured characteristics of soft-rock slip zone and experimental study of its formation mechanism in Boji Mountain large-scale old landslide, Chin. J. Rock Mech. Eng. 32 (7) (2013) 1382–1391 (in Chinese).
[13] B.Y. Zhang, J.H. Zhang, G.L. Sun, Deformation and shear strength of rockfill materials composed of soft siltstones subjected to stress, cyclical drying/wetting and temperature variations, Eng. Geol. 190 (2015) 87–97.
[14] Z. Huang, Z.Q. Jiang, S.Y. Zhu, et al., Influence of structure and water pressure on the hydraulic conductivity of the rock mass around underground excavations, Eng. Geol. 202 (2016) 74–84.
[15] H.H. Zhu, B. Ye, Y.C. Cai, et al., An elasto-viscoplastic model for soft rock around tunnels considering overconsolidation and structure effects, Comput. Geotech. 50 (2013) 6–16.
[16] M.O. Ciantia, R. Castellanza, G.B. Crosta, et al., Effects of mineral suspension and dissolution on strength and compressibility of soft carbonate rocks, Eng. Geol. 184 (2015) 1–18.
[17] T. Hueckel, R. Pellegrini, C. Del Olmo, A constitutive study of thermo-elasto-plasticity of deep carbonatic clays, Int. J. Numer. Anal. Methods Geomech. 22 (7) (1998) 549–574.
[18] G. Rocchi, M. Fontana, M. Da Prat, Modelling of natural soft clay destruction processes using viscoplasticity theory, Geotechnique 53 (8) (2003) 729–745.
[19] S. Kimoto, F. Oka, An elasto-viscoplastic model for clay considering destructuredization and consolidation analysis of unstable behavior, Soil Found. 45 (2) (2005) 29–42.

[20] D.S. Liyanapathirana, J.P. Carter, D.W. Airey, Numerical modeling of nonhomogeneous behavior of structured soils during triaxial tests, Int. J. Geomech. 5 (1) (2005) 10–23.
[21] S.D. Hinchberger, G.F. Qu, Viscoplastic constitutive approach for rate-sensitive structured clays, Can. Geotech. J. 46 (6) (2009) 609–626.
[22] E.Y. Zhu, Y.P. Yao, A structured UH model, in: Constitutive Modeling of Geomaterials, Springer, Berlin, Heidelberg, 2013, pp. 675–689.
[23] Y.P. Yao, A.N. Zhou, Non-isothermal unified hardening model: a thermo-elasto-plastic model for clays, Geotechnique 63 (15) (2013) 1328.
[24] L.C.S.M. Ozelim, J. Camapum de Carvalho, A.L.B. Cavalcante, et al., Novel approach to consolidation theory of structured and collapsible soils, Int. J. Geomech. 15 (4) (2014) 04014064.
[25] M.D. Liu, J.P. Carter, C.S. Desai, Modeling compression behavior of structured geomaterials, Int. J. Geomech. 3 (2) (2003) 191–204.
[26] S. Leroueil, P.R. Vaughan, The general and congruent effects of structure in natural soils and weak rocks, Geotechnique 40 (3) (1990) 467–488.
[27] A. Gens, R. Nova, Conceptual bases for a constitutive model for bonded soils and weak rocks, in: Geotechnical Engineering of Hard Soils-Soft Rocks, vol. 1, 1993, pp. 485–494.
[28] M.D. Liu, J.P. Carter, A structured cam clay model, Can. Geotech. J. 39 (6) (2002) 1313–1332.
[29] A. Asaoka, M. Nakano, T. Noda, Super loading yield surface concept for the saturated structured soils, in: Application of Numerical Methods to Geotechnical Problems, Springer, Vienna, 1998, pp. 233–242.
[30] A. Asaoka, M. Nakano, T. Noda, et al., Delayed compression/consolidation of natural clay due to degradation of soil structure, Soil Found. 40 (3) (2000) 75–85.
[31] A. Asaoka, M. Nakano, T. Noda, Superloading yield surface concept for highly structured soil behavior, Soil Found. 40 (2) (2000) 99–110.
[32] A. Asaoka, Consolidation of clay and compaction of sand, an elastoplastic description, in: Proceedings of the 12th Asian Regional Conference on Soil Mechanics & Geotechnical Engineering, 2003, pp. 1157–1196.
[33] D. Wang, T.H. Kang, Z.Y. Chai, et al., Experimental studies of subsidence and expandability of montmorillonitic soft rock particles under electrochemical treatment, Chin. J. Rock Mech. Eng. 28 (9) (2009) 1876–1883 (in Chinese).
[34] K. Hashiguchi, Subloading surface model in unconventional plasticity, Int. J. Solids Struct. 25 (1989) 917–945.
[35] C. Cekerevac, L. Laloui, Experimental study of thermal effects on the mechanical behaviour of a clay, Int. J. Numer. Anal. Methods Geomech. 28 (3) (2004) 209–228.